HORIZON-EUROHPC-JU-2021-COE-01

The European Centre of Excellence for Engineering Applications

Project Number: 101092621

D2.14 Report on the FLEW Application Use Case

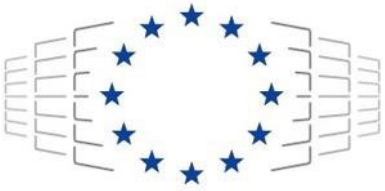

EuroHPC
Joint Undertaking

The EXCELLERAT P2 project has received funding from the European High-Performance Computing Joint Undertaking (JU) under grant agreement No 101092621. The JU receives support from the European Union's Horizon Europe research and innovation programme and Germany, Italy, Slovenia, Spain, Sweden and France.

Work Package:	2	Use-Case Execution
Author(s):	Sergio Pirozzoli	URMLS
	Giulio Soldati	URMLS
	Francesco Salvadore	CINECA
Approved by	Executive Centre Management	17.11.2023
Reviewer	Gregor Weiß	USTUTT
Reviewer	Jonathan Vincent	KTH
Dissemination Level	Public	

Date	Author	Comments	Version	Status
23.10.2023	Giulio Soldati, Sergio Pirozzoli	Full document drafting	V1.0	Draft
25.10.2023	Francesco Salvadore	Format adaptation	V1.1	Ready for peer-review
03.11.2023	Giulio Soldati, Francesco Salvadore	Implementation of review suggestions	V1.2	Ready for second peer-review
13.11.2023	Francesco Salvadore	Implementation of second review suggestions	V1.3	Ready for final submission

List of abbreviations

CFD	Computational Fluid Dynamics
DNS	Direct Numerical Simulation
DR	Drag Reduction
MPI	Message Passing Interface
NPS	Net Power Savings
StTW	Streamwise Travelling Waves
UC	Use Case
WENO	Weighted Essentially Non-Oscillatory
WP	Work Package

Executive Summary

This document presents the progress made in the FLEW Application Use Case UC-6 within reporting period 1 covering the first year of the EXCELLERAT P2 project. Based on the detailed roadmap of the workflow development defined in deliverable D2.1, the workflow of the use case is summarised and the achieved progress with respect to the defined workflow, objectives and success criteria is presented.

In summary, the workflow development for UC-6 has progressed according to the schedule defined in deliverable D2.1. Work has been performed on the individual tasks planned for the first year of the project.

In particular, the tasks of this first phase had the objective of obtaining an initial version of the FLEW code which includes the implementation of all the algorithms necessary for the simulations envisaged in Use Case 6. The application code has been extensively validated by comparing the results in several physical cases known in the literature. In collaboration with WP3, FLEW will now be rewritten and adapted to best benefit from the computing architectures available in the EuroHPC environment.

Table of Contents

Table of Figures

1 Introduction

The quest to reduce fuel consumption and CO_2 emissions in transport has been a powerful driving force for scientific research into flow control methods aimed at reducing the drag exerted by air or water on vehicles. Especially in air transportation, where improving aerodynamic efficiency is essential, drag reduction techniques have potential application for next-generation aircraft design. In cruise conditions, fuel consumption is almost linearly dependent on the aerodynamic drag, and this correlation explains the quest for innovative, technologically realizable approaches to flow control that achieve a reduction in drag. In civil aviation, skin-friction drag accounts for around 50% of the total drag in cruise conditions, thus being a preferential target for research [1]. Most research for skin-friction drag reduction has taken place in the context of parallel flows, in which drag is entirely due to friction. However, the flow over an aircraft wing is a more complex configuration, which involves pressure gradients and shock waves. As a result, aerodynamic drag includes additional contributions besides viscous friction, such as pressure drag, parasitic drag, lift-induced drag and wave drag. In order to reduce fuel consumption and CO_2 emissions, what ultimately matters is reducing the overall drag. The research community is beginning to explore how flow control for skin-friction reduction affects the other drag components [2].

Techniques for turbulent skin-friction drag reduction span from simple passive strategies (e.g., riblets) to active approaches. An example of the latter is the streamwise travelling waves (StTW) of spanwise wall forcing, introduced by Quadrio et al. [3]. This technique is extremely interesting for two reasons: first, it was shown that it can be effective at Reynolds number comparable to those of an aircraft in cruise phase [4]; second, recent studies suggest that this type of flow control aimed at skin friction reduction may also have beneficial effects on wave drag. Specifically, it was shown that the application of spanwise forcing changes the shock-wave position, consequently increasing lift [5]; moreover, this forcing causes stronger expansion in the fore part and a delayed, more intense shock. This is equivalent to an increase of the Mach number on the suction side of the wing, and significantly improves the lift/drag ratio.

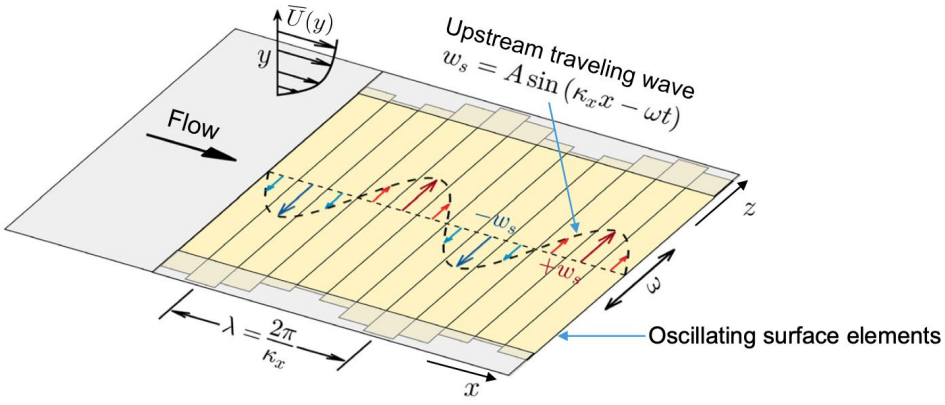

Figure 1: Schematic of the actuation scheme used in [6]: an upstream traveling wave of spanwise velocity is created by synchronously sliding elements (slats) embedded in the surface, interacting with the boundary layer.

The spanwise forcing can be practically realised by using an actuating mechanism, which produces an oscillatory motion of a portion of the wing surface. Such an experiment was carried out by Marusic [6], who did the first experimental measurements of drag reduction induced by oscillatory surface actuation at high Reynolds numbers by installing a customised flow-control

machine. This machine, depicted in Figure 1, can reproduce a discretised facsimile of the streamwise travelling wave, by oscillating 48 slats sinusoidally in the spanwise direction. The sinusoidal oscillation is prescribed by $w_w(x,t) = A\, f(x) \sin(\kappa_x x - \omega t)$, where w_w is the velocity enforced at the wall, A is the maximum forcing amplitude, κ_x is the streamwise wavenumber of the wave, ω its angular frequency, and $f(x)$ is a smoothing function. This experiment showed a drag reduction of 13% at friction Reynolds number $\mathrm{Re}_\tau = 12800$ can be achieved for a flat plate configuration. Figure 2 shows drag reduction and net power saving as a function of the friction Reynolds number achieved with this technique. Referring to Figure 2, the normalised control parameters are defined as $A^+ = A/u_\tau$, $\kappa_x^+ = \kappa_x \nu/u_\tau$, $T_{osc}^+ = 2\pi\frac{u_\tau^2}{\omega\nu}$, where u_τ is the friction velocity.

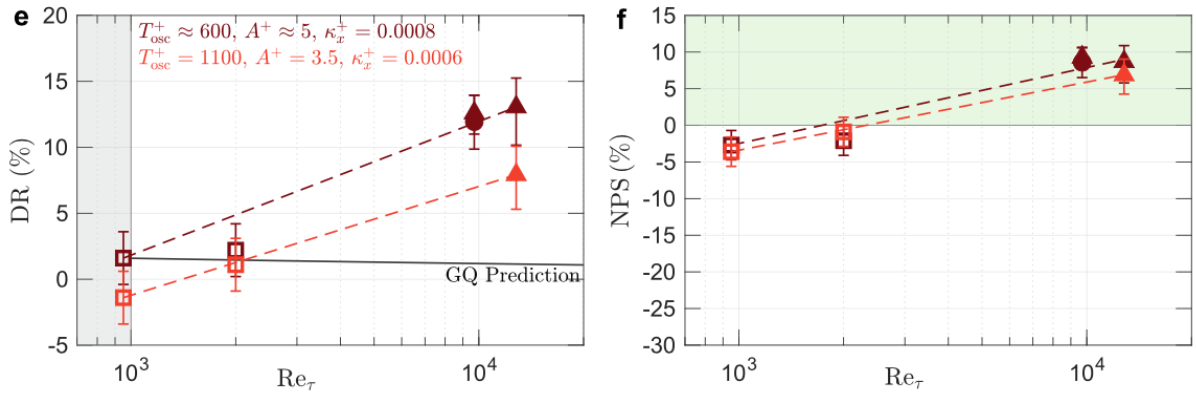

Figure 2: Percentage increase of drag reduction (DR) and net power saving (NPS) with friction Reynolds number for a large-eddy actuation [6].

2 Objectives of the Use Case

Studies carried out so far within skin-friction drag reduction are mostly limited to low-Reynolds-number turbulent flows and elementary geometries, such as flat plates and straight ducts. For these techniques to be exploited in cases of practical interest, it is essential to understand whether the established benefits scale up when these limitations are relaxed. The present work focuses on active flow control for drag reduction, since it generally produces larger effects (which are easier to identify) with respect to passive techniques. Specifically, we consider the StTW of spanwise wall forcing. It was shown that this technique, besides the capability to deliver substantial net savings, can remain effective at Reynolds numbers comparable to those of an aircraft in cruise phase. However, how to assess drag reduction in practical applications, often characterised by curved walls and non-uniform pressure gradients, remains an interesting open challenge.

The aim of this work is to understand how the application of StTW, nominally designed as a device for skin-friction drag reduction, affects the overall aerodynamic drag in a finite wing slab. In detail, we explore the extent to which a localised control for skin-friction reduction interacts with the shock wave and alters the aerodynamic performance of the airfoil. The main value of the asset consists in developing a numerical code, FLEW, which can serve as a tool for the prediction of the optimal wall actuation on wing airfoils under transonic conditions. Numerical simulations will serve to identify optimal operation conditions. The main objectives of the use case are the determination of optimal flow control parameters for flow actuation and

the extension of predictive capabilities of CFD to Reynolds numbers relevant for practical applications.

3 Workflow Description

The workflow we are following to pursue our objectives can be described by the following points:

i) Development of a baseline CPU version of the code FLEW.
ii) Implementation of airfoil boundary conditions and wall actuation.
iii) Code validation in various configurations and flow regimes.
iv) Code restructuring following object-oriented design, aimed to support multiple computing backends.
v) Code porting to multi-GPU architectures oriented to EuroHPC machines.
vi) Validation and benchmarking of restructured/ported code.
vii) Optimisation runs spanning a wide range of parameters to identify optimal operation conditions.
viii) Large scale run for optimised parameters at unprecedented Reynolds numbers.
ix) Post-processing and statistics analyses.
x) Dissemination of results in conference and peer-reviewed journals.

4 Progress Achieved

At present, the first three points of the workflow have been completed.

i) Development of a baseline CPU version of the code FLEW. The code FLEW, based on the work of Pirozzoli [7], solves the compressible Navier-Stokes equations. Compressibility effects, although being crucial in these configurations, have often been neglected in previous simulations. Complex geometries are handled using structured body-fitted meshes in a generalised curvilinear coordinate framework, where the balance equations can be expressed as follows:

$$\frac{1}{J}\frac{\partial \mathbf{Q}}{\partial t} + \frac{\partial \mathbf{F}_j}{\partial \xi_j} = \frac{\partial \mathbf{F}_j^v}{\partial \xi_j}$$

where $\mathbf{Q}$ is the vector of conservative variables, $\mathbf{F}_j$ is the vector of convective fluxes, $\mathbf{F}^v_j$ is the vector of viscous fluxes and J is the Jacobian of the coordinate transformation. Here, we consider stationary grids. A full description of the fluxes' vectors can be found in [8]. A curvilinear body-fitted mesh is first represented in physical space, x_i. Through the transformation $x_i(\xi_j)$ it is then mapped to the computational space, ξ_j, where it can be seen as a regular hexahedron. Non-uniform skewed input cells of the mesh are thus re-stretched into uniform cubical cells. Finite-difference schemes are applied in the computational space to approximate spatial derivatives, which must be reconstructed in the physical space by using the metrics, $\partial\xi_j/\partial x_i$. Since the mesh is directly described in the physical space, first we compute the inverse of the metrics,

$\partial x_i/\partial \xi_j$, by numerically deriving the physical mesh coordinates; then the metrics are obtained with a matrix inversion. To guarantee free-stream preservation, we use the same approximation for both metric and convective derivatives [9].

Space discretisation is based on finite-difference schemes. High-order, low-dissipative numerical schemes are implemented, to guarantee high accuracy and reliability. In smooth regions of the flow, central schemes with a skew-symmetric-like splitting of the convective derivatives are employed. This approach guarantees preservation of kinetic energy in the semi-discrete, inviscid low-Mach-number limit. A computationally effective implementation of convective derivatives cast in split form was proposed by Pirozzoli [10]. The locally conservative formulation allows straightforward hybridisation of central schemes with classical shock-capturing reconstructions. Shock-capturing capabilities rely on Weighted Essentially Non-Oscillatory (WENO) reconstruction of the numerical flux in the proximity of discontinuities. To evaluate the local smoothness of the numerical solution and switch between the energy preserving and the shock capturing discretisation, the code relies on a modified version of the Ducros shock sensor. The viscous terms are expanded to Laplacian form to avoid odd-even decoupling phenomena. The spatial derivatives are approximated in the computational space with central formulas and reconstructed in the physical space by applying the chain-rule. The accuracy order of each scheme can be selected by the user and goes up to eight in the case of central schemes, up to seventh for WENO ones. The system is advanced in time using a three-stage, third order Runge-Kutta scheme [11].

ii) Implementation of airfoil boundary conditions and wall actuation. Other activities have been carried out regarding the correct and efficient implementation of the wake boundary conditions needed to handle the case of airfoil simulations based on C-meshes. The closure of the C-mesh in the wake region results in the generation of a boundary in the computational domain that clearly does not exist in the physical domain. This impasse, if not handled correctly, can lead to numerical errors (i.e., different solutions in the same nodes), to avoid which ad hoc solutions are often used. In our code, no imposition on the solution is enforced. Moreover, wake boundary conditions activities include addition of point-to-point send/received message-passing instructions, on top of the baseline Cartesian Message Passing Interface (MPI) topology, as well as suitable tagging of the boundary nodes for the correct enforcement of the no-slip wall boundary conditions on the airfoil. Since we are interested in turbulent flows, we implemented a numerical tripping to initiate the turbulent boundary layer. Following the work of Schlatter and Örlü [12], the tripping is implemented as a weak random volume force acting in wall-normal direction, on the suction and the pressure side of the airfoil. The flow control technique for drag reduction is based on a spanwise forcing at the wing surface. From a numerical point of view, this means implementing customised wall boundary conditions to impose StTW of spanwise velocity. StTW are applied to a portion of the suction side of the wing, according to

$$w_w(x,t) = A f(x) \sin(\kappa_x x - \omega t),$$

where A is the maximum forcing amplitude, and κ_x and ω are the spatial and temporal frequencies of the wave. A smoothing function $f(x)$ is used to raise the spanwise velocity at the initial position of the actuated region and then return it to zero at the final position. The purpose of this work is to precisely identify the optimal flow control parameters.

iii) Code validation in various configurations and flow regimes. At this stage, extensive validation activities of the FLEW software have been carried out. First, we verified that the code is able to preserve kinetic energy at a discrete level in the inviscid low-Mach-number limit.

To this purpose, we considered the time-reversibility benchmark proposed by Duponcheel et al. [13]. The test was performed using different meshes: Cartesian, curvilinear, randomised. In all cases, total kinetic energy remains perfectly constant over time and the initial conditions are exactly recovered. Figure 1 refers to the curvilinear case: on the left we report the initial and final conditions in terms of iso-surface of Q-criterion; on the right the time evolution of total kinetic energy and total enstrophy is shown.

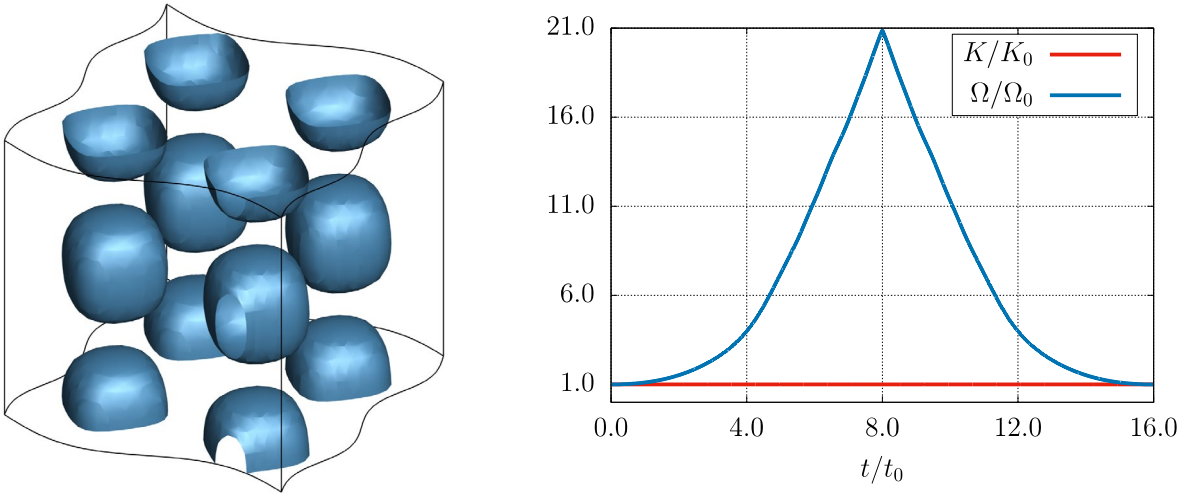

Figure 3 Time-reversibility benchmark on a curvilinear grid: initial and final conditions in terms of iso-surface of Q-criterion (left); time evolution of total kinetic energy, in red, and total enstrophy, in blue (right).

Then, we focused on validation in the presence of imposed pressure gradients due to surface curvature. For that purpose, we considered the classical study by Moser & Moin [14], in which pressure-driven flow between two concentric cylinders was simulated. The same flow configuration was recently used by Brethouwer [15] as benchmark. Some code adaptations were required to have a provision for radial variation of the imposed pressure gradient. Results have shown perfect agreement in terms of mean values and variances. We show in Figure 4 the mean velocity profile in local wall units (left) and the RMS of velocity fluctuations (right).

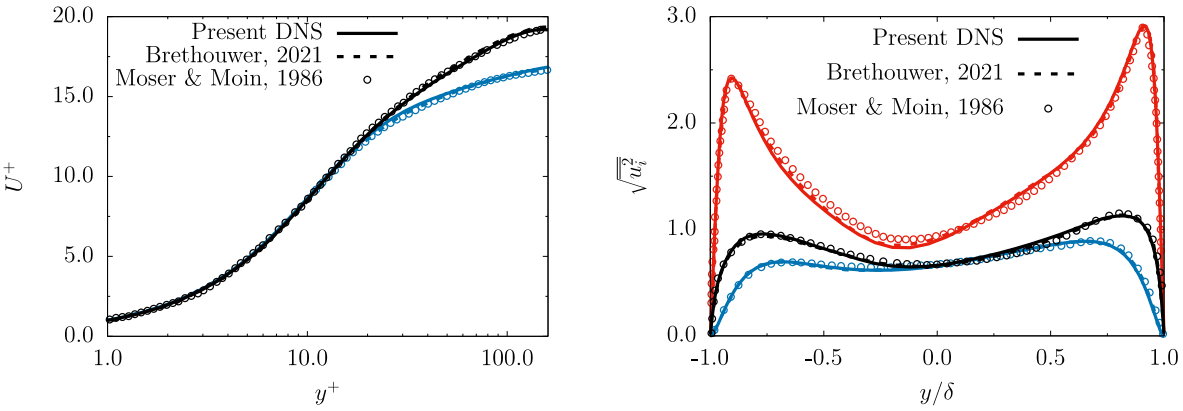

Figure 4: Turbulent curved channel flow: mean velocity profile in local wall units (left); RMS of velocity fluctuations (right).

We also focused also on high Mach number configurations, namely the supersonic ramp flow, both in the laminar and turbulent regimes. Regarding the laminar case, we considered the recent work of Cao et al. [16]. The results in terms of skin friction coefficient, wall pressure and Stanton number are in excellent agreement with the reference values. Regarding the turbulent case, we considered the computational work of Wu and Martin [17] and the experimental work of Bookey et al. [18]. The mean values of wall pressure, velocity and Van Driest transformed velocity proved to be in great agreement, as well as for pressure fluctuations. Figure 5 shows the mean wall pressure distribution along the ramp (left) and the velocity profile at two different locations, before and after the ramp corner.

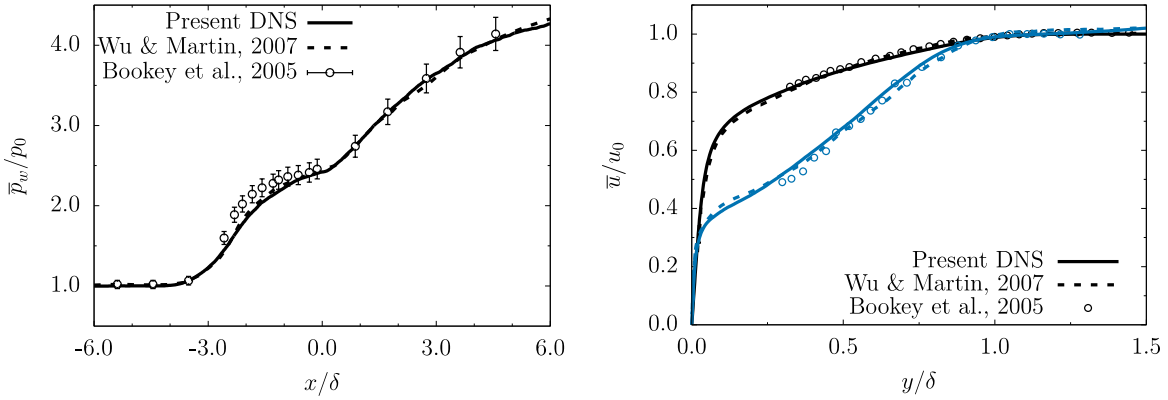

Figure 5: Supersonic turbulent ramp flow: mean wall pressure distribution (left); mean velocity profiles (right) located upstream of ramp corner, in black, and downstream, in blue.

As first step of the airfoil flow validation, we considered the work of Swanson [19], who simulated a class of laminar flows around the NACA 0012 airfoil. This class of flows is often used as test case for high-order numerical schemes, and to evaluate accuracy, stability and convergence of numerical solution of the Navier-Stokes equations. Specifically, we focused on a transonic flow at Mach number 0.8, Reynolds number 500 (based on the chord length) and angle of attack 10°. The pressure coefficient (left) and the skin-friction coefficient (right) distribution are presented in Figure 6.

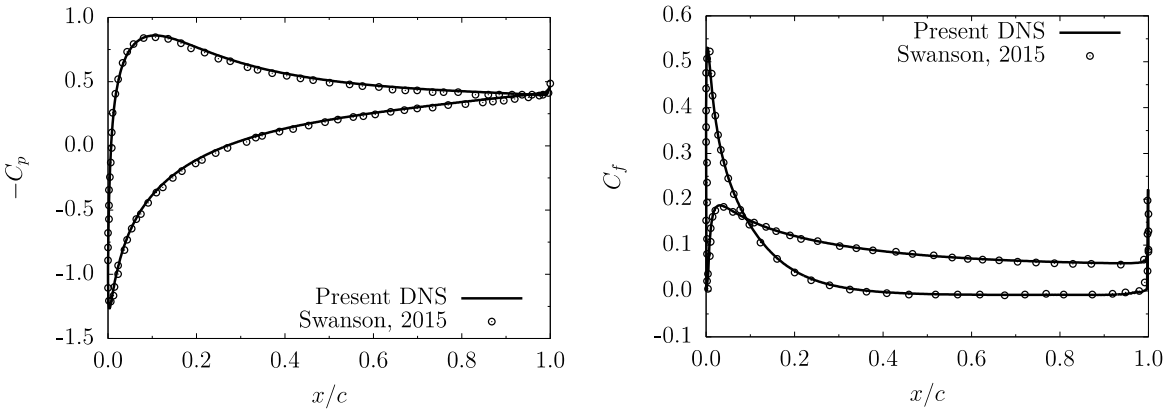

Figure 6: Laminar flow around a NACA 0012 airfoil: pressure coefficient distribution (left); skin-friction coefficient distribution (right).

Finally, the simulation of a transonic flow over a supercritical profile is currently running at conditions comparable to those of interest, nominally Mach number 0.7, Reynolds number $3 \cdot 10^5$ and angle of attack 4°. The flow conditions, profile geometry and computational grid are the same as those considered by Quadrio et al. [2]. Figure 7 shows the velocity magnitude on a wall-parallel plane on the suction side at $y^+=15$, while Figure 8 shows the numerical Schlieren on a streamwise wall-normal plane.

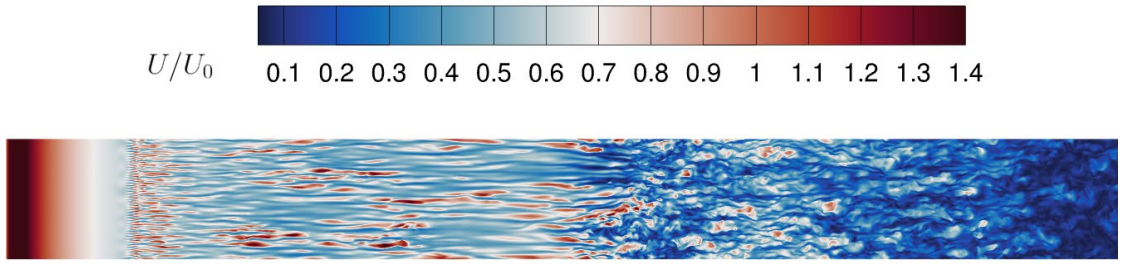

Figure 7: Turbulent flow around a supercritical airfoil: instantaneous field of the velocity magnitude on a wall-parallel plane on the suction side at $y^+=15$.

Figure 8: Turbulent flow around a supercritical airfoil: instantaneous field of the numerical Schlieren on a streamwise wall-normal plane.

5 Conclusion

The activities reported in this deliverable are carried out in synergy with the activities of WP3 and WP4. In particular, deliverable D3.1 reports the ongoing technological activities intrinsically linked to the activities considered in this D2.14. The code validation reported in this D2.14 refers to a version of the code capable of running on CPUs and featuring a first implementation for NVIDIA GPUs, and is already usable for production. At the same time, in WP3, a complete rewriting of the code is underway using an object design similar to that of the STREAmS community code (https://github.com/STREAmS-CFD/STREAmS-2), which shares the same developers as FLEW ones. The object-oriented design guarantees better programmability/maintainability of the code and above all is oriented towards support of multiple computational backends. In particular, efforts will be aimed at supporting architectures present in the EuroHPC context, i.e., AMD GPUs, in addition to NVIDIA GPUs, using different programming

paradigms. The possibility of unifying, even partially, FLEW and STREAmS-2 is currently under investigation. For more details, please refer to D3.1. FLEW development will be also performed in the context of WP4, especially concerning in situ visualisation functionalities.
The final version of FLEW will be benchmarked on different EuroHPC architectures and used for production runs. In particular, we will proceed with the simulations of transonic flow around supercritical airfoils. Specifically, first step will be to carry out about a hundred preliminary medium sized Direct Numerical Simulation (DNS) to identify the optimal parameters of flow control via travelling waves. The second step will be to perform a few large-scale DNS runs for both uncontrolled and controlled case.

6 References

[1] Ricco, P., Skote, M., & Leschziner, M. A. (2021). A review of turbulent skin-friction drag reduction by near-wall transverse forcing. *Progress in Aerospace Sciences*, *123*, 100713.
[2] Quadrio, M., Chiarini, A., Banchetti, J., Gatti, D., Memmolo, A., & Pirozzoli, S. (2022). Drag reduction on a transonic airfoil. *Journal of Fluid Mechanics*, *942*, R2.
[3] Quadrio, M., Ricco, P., & Viotti, C. (2009). Streamwise-travelling waves of spanwise wall velocity for turbulent drag reduction. *Journal of Fluid Mechanics*, *627*, 161-178.
[4] Gatti, D., & Quadrio, M. (2016). Reynolds-number dependence of turbulent skin-friction drag reduction induced by spanwise forcing. *Journal of Fluid Mechanics*, *802*, 553-582.
[5] Banchetti, J., Luchini, P., & Quadrio, M. (2020). Turbulent drag reduction over curved walls. *Journal of Fluid Mechanics*, *896*, A10.
[6] Marusic, I., Chandran, D., Rouhi, A., Fu, M. K., Wine, D., Holloway, B., ... & Smits, A. J. (2021). An energy-efficient pathway to turbulent drag reduction. *Nature Communications*, *12*(1), 5805.
[7] Pirozzoli, S. (2011). Stabilized non-dissipative approximations of Euler equations in generalized curvilinear coordinates. *Journal of Computational Physics*, *230*(8), 2997-3014.
[8] Chandravamsi, H., Chamarthi, A. S., Hoffmann, N., & Frankel, S. H. (2023). On the application of gradient based reconstruction for flow simulations on generalized curvilinear and dynamic mesh domains. *Computers & Fluids*, *258*, 105859.
[9] Visbal, M. R., & Gaitonde, D. V. (2002). On the use of higher-order finite-difference schemes on curvilinear and deforming meshes. *Journal of Computational Physics*, *181*(1), 155-185.
[10] Pirozzoli, S. (2010). Generalized conservative approximations of split convective derivative operators. *Journal of Computational Physics*, *229*(19), 7180-7190.
[11] Spalart, P. R., Moser, R. D., & Rogers, M. M. (1991). Spectral methods for the Navier-Stokes equations with one infinite and two periodic directions. *Journal of Computational Physics*, *96*(2), 297-324.
[12] Schlatter, P., & Örlü, R. (2012). Turbulent boundary layers at moderate Reynolds numbers: inflow length and tripping effects. *Journal of Fluid Mechanics*, *710*, 5-34.
[13] Duponcheel, M., Orlandi, P., & Winckelmans, G. (2008). Time-reversibility of the Euler equations as a benchmark for energy conserving schemes. *Journal of Computational Physics*, *227*(19), 8736-8752.
[14] Moser, R. D., & Moin, P. (1987). The effects of curvature in wall-bounded turbulent flows. *Journal of Fluid Mechanics*, *175*, 479-510.
[15] Brethouwer, G. (2022). Turbulent flow in curved channels. *Journal of Fluid Mechanics*, *931*, A21.
[16] Cao, S., Hao, J., Guo, P., Wen, C. Y., & Klioutchnikov, I. (2023). Stability of hypersonic flow over a curved compression ramp. *Journal of Fluid Mechanics*, *957*, A8.

[17] Wu, M., & Martin, M. P. (2007). Direct numerical simulation of supersonic turbulent boundary layer over a compression ramp. *AIAA journal*, *45*(4), 879-889.
[18] Bookey, P., Wyckham, C., Smits, A., & Martin, P. (2005). New experimental data of STBLI at DNS/LES accessible Reynolds numbers. In *43rd AIAA Aerospace Sciences Meeting and Exhibit* (p. 309).
[19] Swanson, R. C., & Langer, S. (2016). Steady-state laminar flow solutions for NACA 0012 airfoil. *Computers & Fluids*, *126*, 102-128.